第 48 卷 第 9 期/2021 年 5 月/中国激光 研究论文

中国激光

基于膜片式 EFPI 光纤麦克风的声源定位系统

夏振杰[1]，刘强[2]，李昂[1]，刘悦莹[1]，荆振国[2]，彭伟[2*]

[1]大连理工大学光电工程与仪器科学学院，辽宁 大连 116024；

[2]大连理工大学物理学院，辽宁 大连 116024

摘要 提出一种采用激光器频率调制准连续相移干涉实现膜片式光纤声传感器阵列同时解调的技术。通过调制光栅 Y 分支(MG-Y)可调谐激光器的快速频率调谐引入相移，4 个具有 π/2 相位偏置的光频率按顺序切换，产生准连续的正交相移信号。基于五步相移算法，任意 5 个相邻相移信号用于相位恢复，由于没有机械运动部件，实现了高速稳定的相位解调。该系统的相位采样率(600 kHz)取决于频率调制速度。实验结果表明，通过调整激光器输出频率，可以正确解调宽腔长范围的非本征 Fabry-Perot 干涉(EFPI)传感器。此外，构建了一个紧凑的多点声传感阵列系统，实现了声源定位应用。

关键词 测量；相位测量；相移干涉术；调制光栅 Y 分支激光器；光纤麦克风；声源定位

中图分类号 TP212.9 **文献标志码** A **doi**：10.3788/CJL202148.0910002

1 引 言

光纤声传感器具有体积小、抗电磁干扰、频率响应宽、在恶劣环境下具有良好性能等特点，在光声内窥镜的超声检测[1]、气体绝缘开关设备的局部放电检测[2]、气体微泄漏的远程监测[3]、变压器油中溶解气体检测[4]、液氮中声发射波的速度测量[5]等领域发挥着重要作用。在过去的二十年里，各种类型的光纤声传感器得到了广泛的研究和开发，包括光纤布拉格光栅(FBG)声传感器[6]、光纤激光声传感器[7]和干涉式声传感器(Sagnac[8]、Mach-Zehnder[9]、Michelson[10]和 Fabry-Perot[11-12])。其中，基于膜片的非本征 Fabry-Perot 干涉(EFPI)式声传感器以高灵敏度和具有反射型传感器结构而备受关注，膜片随着所施加的声压振动，导致输出干涉光的强度或相位变化。

基于正交点(Q 点)的强度检测是 EFPI 声传感器应用最广泛的解调技术之一[13]。高性能 Q 点稳定是实现声学检测稳定有效的关键[14-15]。强度解调方法可以直观地反映所施加的声音信号，但是检测到的声压动态范围受到限制，检测到强声信号时会发生信号失真。此外，不同传感器的 Q 点易受外部环境波动的影响，消除了多路复用和多点检测的可能性。相反，诸如相位产生载波(PGC)解调之类的相位解调方案具有更大的动态范围和更好的稳定性。PGC 解调方法[16]通常需要压电陶瓷换能器(PZT)来生成相位载波，这会使系统体积庞大。而且，PZT 的机械特性会导致有限的频率响应范围。2019 年，Liu 等[17]设计了一种共路双波长相位解调技术，实现了 250 kHz 的相位采样率。干涉光谱的直流(DC)分量在整个测量过程中被认为是恒定的，这在实际应用中会带来解调误差[18]。对于三波长相位解调方案，DC 分量可以在线补偿，从而使其更加稳定，但是需要额外的可调谐激光器和光电探测器(PD)[18]。

随着快速可调谐激光器的发展，频率或波长调制相移干涉技术(PSI)成为一种很有潜力的高速相位恢复方法[19-21]。通过可调激光器的频率或波长调谐引入目标正交相移，从而避免了诸如 PZT 之类的移相器引起的非线性误差。并且不同腔长的 EFPI 传感器可以分别计算相移值，实现同时解调，为多路复用和多点检测提供了可能性。二维声源定位是多点声探检测最典型的应用之一。由于传统的电声传

收稿日期：2020-10-20；**修回日期**：2020-11-19；**录用日期**：2020-12-08

基金项目：国家自然科学基金(61727816，61520106013)、中央大学基础研究基金(DUT18ZD215)

*E-mail：wpeng@dlut.edu.cn

感器无法在液氮等恶劣环境下工作[5]，近年来，基于光纤声传感器的声源定位方法引起了广泛的研究兴趣[22-24]。到目前为止，大多数多点光纤声学检测系统都是基于 FBG 传感器阵列[25-26]，因为它们在波长域具有多路复用特性。然而，FBG 声传感器存在灵敏度低的问题。而光纤 EFPI 声传感器结合高性能、灵活的多点解调技术，因具有探头式的结构和高灵敏度的优势更适合用于声源定位。

本文使用调频准连续 PSI(FMQC-PSI)方法对光纤麦克风进行相位解调。依次连续地切换具有 π/2 弧度相位偏置的 4 个光频率，生成准连续正交相移信号，获得更高的相位采样率。基于稳定的五步相移算法[27]，利用任意 5 个相邻的强度信号来恢复相位值。通过调节 4 个光频率，可以有效地解调具有宽腔长范围的 EFPI 声传感器。将基于 FMQC-PSI 的单点声学检测系统扩展到多点声学检测系统，成功地实现了二维(2D)声源定位。

2 传感器制作和解调原理

2.1 膜片式 EFPI 光纤麦克风

图 1 为 EFPI 光纤麦克风的制作过程。首先，如图 1(a)所示，将引入光纤放入内径为 126 μm 的毛细管中；接着，将图 1(a)所示结构依次放入内径为 1.81 mm 和 3.4 mm 的毛细管中，并用紫外光固化胶(UV 胶)进行粘结，然后在紫外光下照射固化，结果如图 1(b)和(c)所示；最后，通过 UV 胶将聚对苯二甲酸乙二醇酯(PET)膜片粘附在毛细管的端面，并在紫外光下照射固化，形成的光纤麦克风结构如图 1(d)所示。其中 PET 膜片的厚度为 6 μm，直径为 3.4 mm。

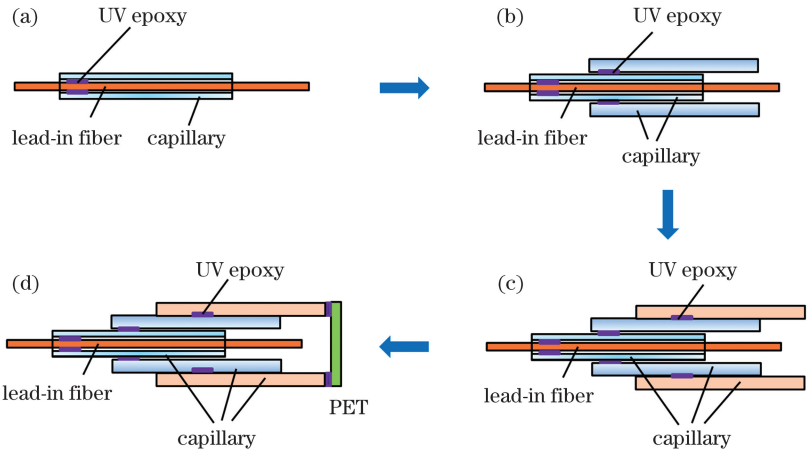

图 1 EFPI 光纤麦克风的制造过程示意图

Fig. 1 Schematic of fabrication process of the EFPI optical fiber microphone

2.2 EFPI 光纤麦克风腔长解调原理

所提 FMQC-PSI 相位解调系统如图 2(a)所示。采用全半导体可编程调制光栅 Y 分支(MG-Y)可调谐激光器(AOC，ATLS7500)作为移相器，它的频率扫描范围为 191.316～196.328 THz，具有平坦的强度输出[17]。由于没有机械运动部件，这种无机械运动的扫频源具有高速和高稳定性的优点[28-30]，此外，它还可以集成到一个紧凑型的系统中，光频率转换由注入电流控制。利用实验室建立的自动校准系统来获得频率调谐的查找表[17]，通过现场可编程门阵列(FPGA)实现稳定的频率控制和同步数据采集，采用具有 PET 膜片的 EFPI 声传感器对系统进行性能测试。

具有 π/2 弧度相位偏置的 4 个光频率依次切换，从而产生如图 2(b)所示的圆形相移循环。对于 EFPI 声传感器，在特定光频率下的反射强度可以表示为

$$I(\nu)=A+B\cos\left[\frac{4n\pi\cdot\nu}{c}L+\varphi_0\right], \tag{1}$$

式中：A 为干涉条纹的直流分量；B 为反射干涉光谱的相干包络；ν 为光学频率；c 为真空中的光速；φ_0 为初始相位，是常数；n 为 EFPI 腔的折射率，$n=1$；L 为 EFPI 传感器的腔长。根据(1)式，为了引入 π/2 相位偏差，频移可计算为

$$\Delta\nu=\frac{c}{8nL}。 \tag{2}$$

将 ν_1 设置为固定的光频率($\nu_1=191.316$ THz)，其他 3 个工作频率可以根据(2)式确定。由于这种特意的频率设置，每两个相邻的调频相移信号之间就满足正交相位条件，利用高性能的相移算法可以计算出由施加的声压调制的时变相位信号。到目前为止，已经研究了各种相移算法以满足不同应用需求[31]，包括 4 步算法[32]、改进的 2+1 算法[33]、5 步

算法[27]等。为了获得较高的相位恢复精度和容忍相移误差，在这项工作中采用五步相移算法。对于任意 5 个相邻的相移信号，它们的强度映射为

$$\begin{cases} I_1 = A + B\cos\left[\dfrac{4n\pi\cdot\nu_1}{c}L + \varphi_0 - \pi\right] \\ I_2 = A + B\cos\left[\dfrac{4n\pi\cdot\nu_2}{c}L + \varphi_0 - \dfrac{\pi}{2}\right] \\ I_3 = A + B\cos\left[\dfrac{4n\pi\cdot\nu_3}{c}L + \varphi_0\right] \\ I_4 = A + B\cos\left[\dfrac{4n\pi\cdot\nu_4}{c}L + \varphi_0 + \dfrac{\pi}{2}\right] \\ I_5 = A + B\cos\left[\dfrac{4n\pi\cdot\nu_1}{c}L + \varphi_0 + \pi\right] \end{cases}。 \tag{3}$$

相应的相位值 Φ 可计算为

$$\Phi = \arctan\left[\frac{2(I_2 - I_4)}{2I_3 - I_1 - I_5}\right]。 \tag{4}$$

相位差 $\Delta\Phi$ 表示施加的声信号引起的相位变化。图 2(c)为频率调谐和相位恢复的时序图，依次切换 4 个光频率，并同步获取相应的光强度，其中光频率的切换时钟为 600 kHz。任意 5 个相邻的相移信号都可以计算 $\Delta\Phi$，从而在连续频率调制期间实现 600 kHz 的相位采样率。此外，反正切运算可能会导致相位跳变，因而在相位跳变点进行了相位补偿[34]，即使声信号引起的相位调制大于 π，也能正确恢复动态信号。

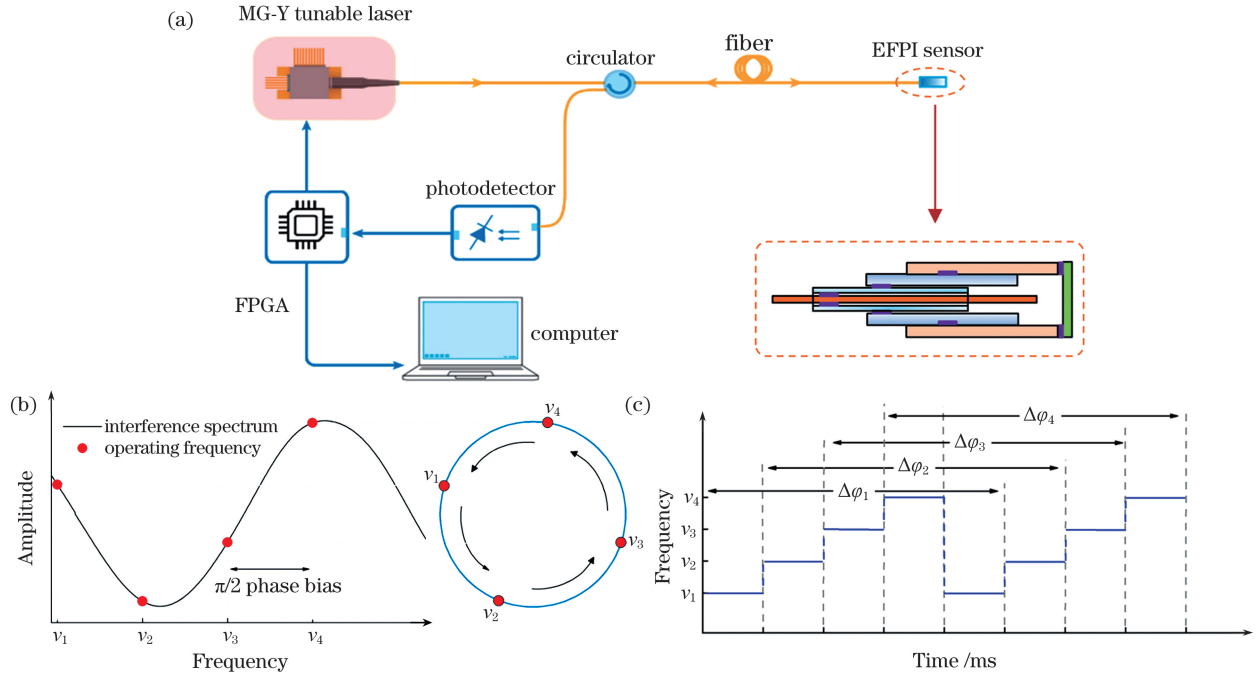

图 2　基于 FMQC-PSI 方法的声解调系统。(a)调频准连续相移干涉测量系统示意图；(b)具有 π/2 相位偏置的 4 个工作频率生成的准连续正交相移信号；(c)频率调谐和相位恢复时序图

Fig. 2　Acoustic demodulation system based on FMQC-PSI method. (a) Schematic of the proposed FMQC-PSI system; (b) generated quasi-continuous quadrature phase shifting signals using four operating frequencies with π/2 phase bias; (c) timing diagram of the frequency tunning and phase retrieval

3　实验结果与讨论

3.1　单点声学检测实验

使用图 2(a)所示的 FMQC-PSI 系统进行单点声学检测来评估其解调性能，测试了腔长为 279.502 μm 的基于 PET 膜片的 EFPI 光纤麦克风。首先利用 MG-Y 激光器进行线性频率扫描，得到图 3(a)所示的干涉光谱，根据干涉光谱得到绝对腔长。扫描范围为 191.316～196.328 THz，光频率间隔为 1 GHz。然后计算出用于产生正交相位偏置的频率偏移为 134 GHz，因此 4 个工作频率分别为 191.316 THz、191.450 THz、191.584 THz、191.718 THz。通过将函数发生器(RIGOL，DG1022)与扬声器(SANSUI，T5)相连，用来产生声信号。首先，产生频率为 3 kHz 的连续正弦波，图 3(b)为与 4 个工作光学频率相对应的时域波形，图 3(c)为恢复的相位信号。然后，调节函数发生器的输出电压，以增大施加的声压，如图 3(d)和图 3(e)所示，尽管对应于 ν_1～ν_4 的强度信号已无法正确反映实际施加的声信号，但解调后的相位信号

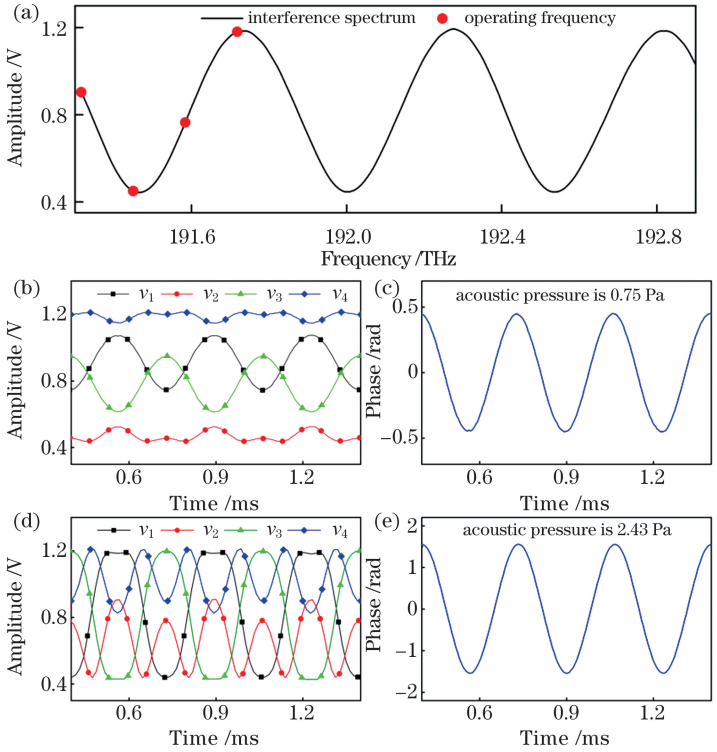

图 3 腔长为 279.502 μm 的 EFPI 光纤麦克风解调结果。(a)通过线性频率扫描获得的干涉频谱和 4 个选定的工作频率；(b)～(e)4 个工作频率对应的时域波形和在不同声压下获取的相位信号

Fig. 3 Demodulation results of the EFPI optical fiber microphone with a cavity length of 279.502 μm. (a) Interference frequency spectrum obtained by linear frequency scanning and the four selected operating frequencies; (b)-(e) time-domain waveforms corresponding to the four operating frequencies and the retrieved phase signals under different acoustic pressures

仍呈现出良好的正弦波形，这表明 FMQC-PSI 系统在检测强声信号方面的优势。图 4 为当输入声压信号的频率为 3 kHz、声压为 2.43 Pa 时，传感器输出信号的功率谱，信噪比(SNR)为 76.8 dB，系统具有 25.4 dB 的本底噪声。

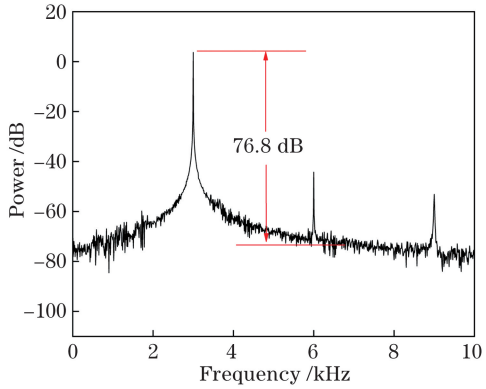

图 4 在频率为 3 kHz、声压为 2.43 Pa 下传感器输出的功率谱

Fig. 4 Output power spectrum of the sensor under 2.43 Pa acoustic pressure and 3 kHz frequency

当固定声信号频率为 3 kHz，通过调节信号发生器的输出电压，施加的声压幅值在 0.75 Pa 和 2.43 Pa 之间变化，得到传感器的输出响应，如图 5(a)所示，传感器的灵敏度为 0.63 rad/Pa，具有良好的线性度($R^2 \geqslant 0.997$)。控制声信号的频率从 1 kHz 逐渐变化到 10 kHz，得到传感器的频率响应曲线，结果如图 5(b)所示。

对于传统的 PGC 解调方法，为了保持较高的解调精度，调制深度 C 具有一个最佳值，通常为 2.37 或 2.63[35]。更换传感器探头时需要重新校准调制深度，这很不方便。对于所提 FMQC-PSI 解调方法，为了解调不同腔长的传感器，需要校准 4 个工作频率。采用 1 GHz 步长的线性频率扫描获得干涉谱并计算腔长，然后根据(2)式选择具有正交相位偏置的 4 个工作频率。此校准过程只需要几秒钟，不需要额外的设备，校准过程非常简单和快速。所提系统能正确解调不同腔长、不同频率的 EFPI 传感器，所测试的 EFPI 传感器的腔长分别为 33.518 μm、136.534 μm、494.833 μm 和 745.504 μm，检测到的声波频率为 1～15 kHz，如图 6 所示。该 FMQC-PSI 解调方法为光纤干涉声传感提供了一个紧凑、通用、高速的相位解调系统。

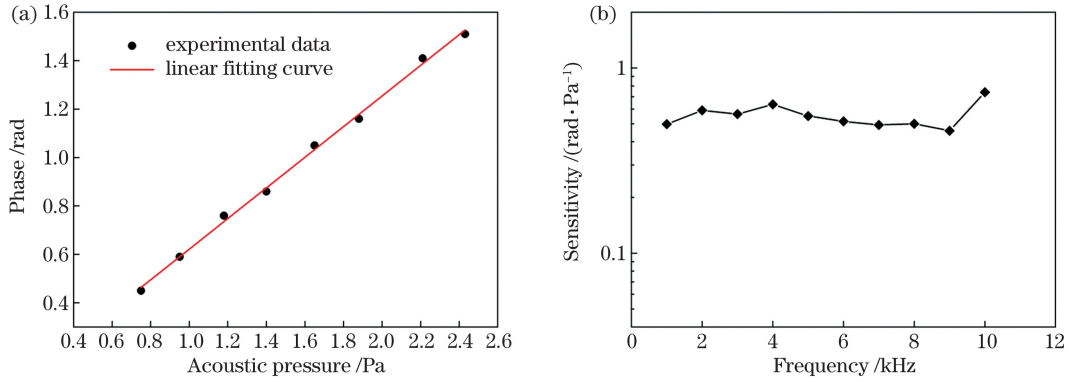

图 5　传感器响应。(a)声压响应曲线;(b)频率响应特性曲线

Fig. 5　Sensor response. (a) Sound pressure response curve; (b) frequency response characteristic curve

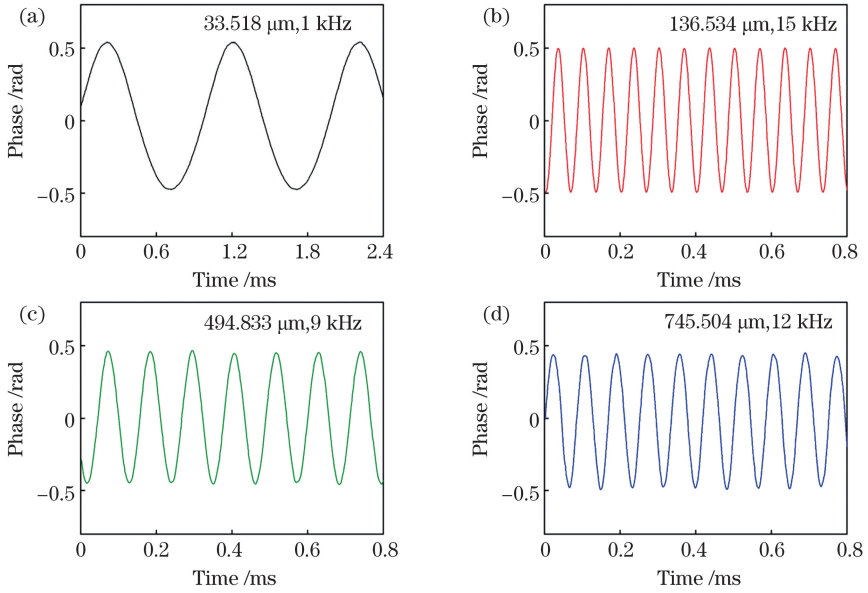

图 6　基于不同腔长的 EFPI 声传感器的解调结果。(a)腔长为 33.518 μm 传感器解调的 1 kHz 相位波形;(b)腔长为 136.534 μm 传感器解调出的 15 kHz 相位波形;(c)腔长为 494.833 μm 传感器解调的 9 kHz 相位波形;(d)腔长为 745.504 μm 传感器解调出的 12 kHz 相位波形

Fig. 6　Demodulated results of EFPI acoustic sensor with different cavity lengths. (a) 1 kHz phase waveform demodulated by sensor with cavity length of 33.518 μm; (b) 15 kHz phase waveform demodulated by sensor with cavity length of 136.534 μm; (c) 9 kHz phase waveform demodulated by sensor with cavity length of 494.833 μm; (d) 12 kHz phase waveform demodulated by sensor with cavity length of 745.504 μm

3.2　二维声源定位实验

将基于 FMQC-PSI 相位解调方案的单点声学检测系统扩展到多点声学检测系统,并进行二维声源定位,如图 7 所示。将 4 个腔长相同[(135.122±1)μm]的 EFPI 声传感器放置在两个正交轴上,坐标分别为传感器 1(45 cm ,0 cm)、传感器 2(0 cm、45 cm)、传感器 3(−45 cm,0 cm)、传感器 4(0 cm,−45 cm)。单个 MG-Y 激光器用于为每个传感器探头生成准连续正交相移信号,每个传感通道仅需要一个 PD。同时获取对应于每个传感通道的强度数据,以进行相位恢复,不会出现重叠或串扰。

使用双曲线定位算法[36]来估计声源位置。利用两对传感器沿正交轴测得的到达时间差(TDOA)来确定两条双曲线,它们的交点为声源位置(x,y):

$$\begin{cases}\dfrac{x^2}{a_{\mathrm{m}}}-\dfrac{y^2}{b_{\mathrm{m}}}=1\\ \dfrac{y^2}{a_{\mathrm{n}}}-\dfrac{x^2}{b_{\mathrm{n}}}=1\end{cases},\tag{5}$$

其中

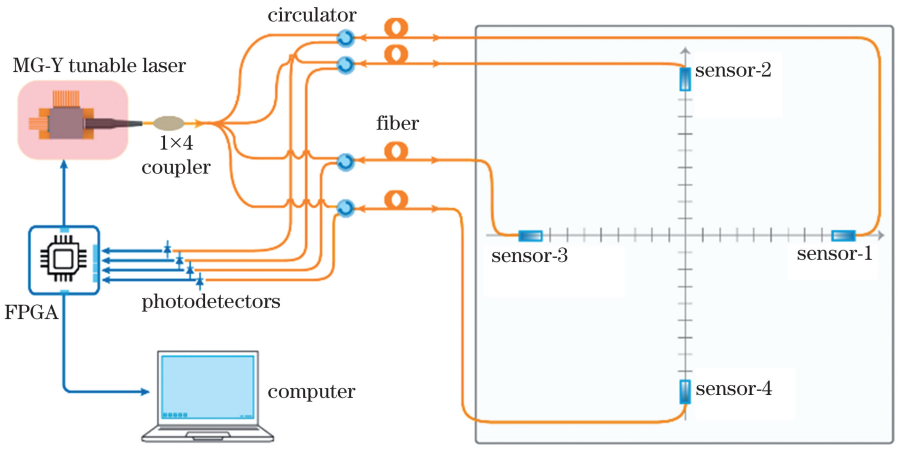

图 7　四传感器声源定位系统示意图

Fig. 7　Schematic of the four-sensor sound source localization system

$$\begin{cases} a_{\mathrm{m}}=v_{\mathrm{s}}\cdot\dfrac{\Delta t_{13}}{2},a_{\mathrm{n}}=v_{\mathrm{s}}\cdot\dfrac{\Delta t_{24}}{2} \\ b_{\mathrm{m}}^2=d^2-a_{\mathrm{m}}^2,b_{\mathrm{n}}^2=d^2-a_{\mathrm{n}}^2 \\ \Delta t_{13}=t_3-t_1,\Delta t_{24}=t_4-t_2 \end{cases}, \tag{6}$$

式中：空气中的声速 v_{s} 为 340 m/s；t_1、t_2、t_3、t_4 为声波到达传感器的时间；Δt_{13} 为传感器 1 和传感器 3 之间的 TDOA，Δt_{24} 为传感器 2 和传感器 4 之间的 TDOA；d 为传感器与原点之间的距离，在本实验中为 45 cm。当点声源置于(30 cm，−15 cm)坐标处时，对应于 4 个传感器的典型时域波形如图 8 所示，可以计算出传感器 1 和传感器 3 之间的时差为 1.614 ms，传感器 2 和传感器 4 之间的时差为−0.763 ms，声源位置估计为(30.01 cm，−15.82 cm)，与实际位置(30 cm，−15 cm)非常吻合。

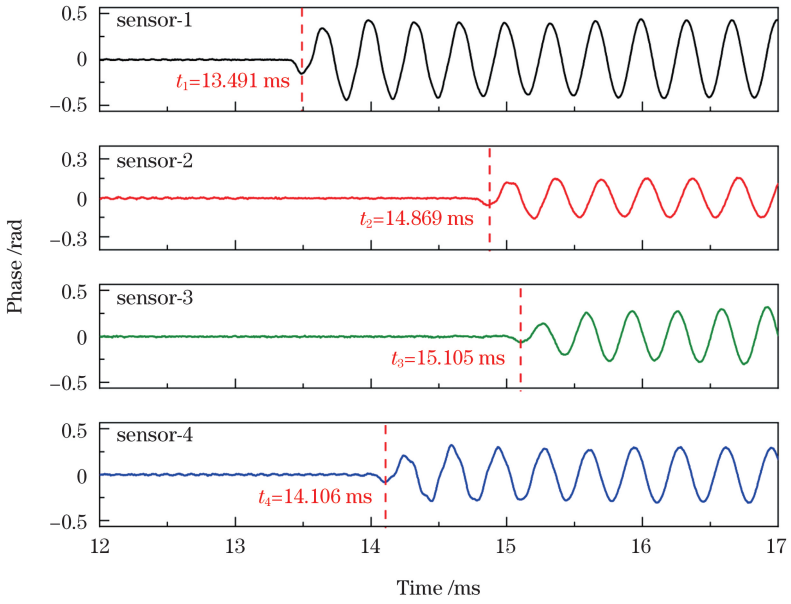

图 8　当点声源置于(30 cm，−15 cm)时，4 个传感器系统检测到的典型时域波形

Fig. 8　Typical time-domain waveforms detected by the four sensor systems when the point sound source is placed at (30 cm, −15 cm)

在 25 个不同位置进行了 6 次重复测量，来测试该系统的定位精度。定位结果如图 9 所示，其中 4 个传感器位置标记为实心圆，实际点声源位置标记为圆圈，估计的声源位置标记为叉。可以发现，在相同声源位置，定位结果具有很高的一致性，所有测量的定位误差均不大于 1.98 cm。实际上，估计位置与实际位置之间的偏差部分是传感器和点声源的放置位置误差引起的。二维声源定位实验证明，FMQC-PSI 相位解调方案在多点声学检测中具有有效性和优越性。

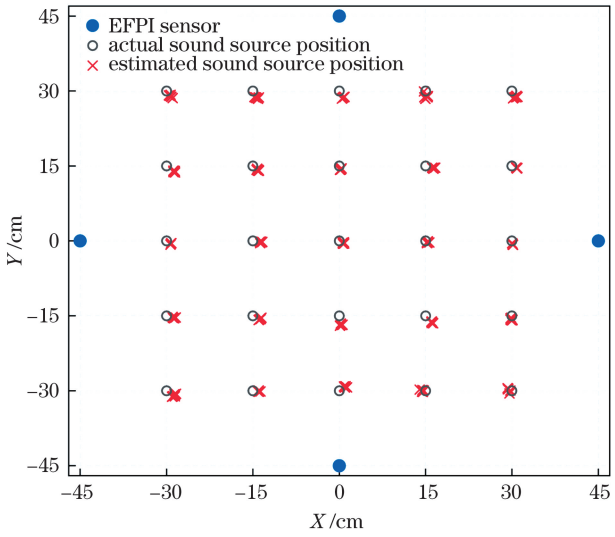

图 9 在 25 个不同位置进行 6 次重复测量

Fig. 9 Six repeated measurements at 25 different positions

4 结 论

采用一种调频正交相移解调技术实现了对膜片式 EFPI 光纤麦克风的相位解调，并演示了它在声源定位中的应用。通过对 4 个具有 π/2 相位差的激光频率进行顺序调制，产生准连续相移信号。相位采样率取决于激光器的频率调谐速率，达 600 kHz。由于 EFPI 声学传感器具有较宽的频率调谐范围(191.316～196.328 THz)，通过调整 4 个激光频率的具体数值，可以解调不同腔长(33.518～745.504 μm)的 EFPI 光纤麦克风。此外，通过空分复用，可以很容易地实现多个声传感器的同时解调。构建了一个紧凑的四传感器 FMQC-PSI 系统用于二维声源定位，实验结果证明了其的有效性。

参 考 文 献

[1] Li G Y, Guo Z D, Chen S L. Miniature probe for forward-view wide-field optical-resolution photoacoustic endoscopy[J]. IEEE Sensors Journal, 2019, 19(3): 909-916.

[2] Ma G M, Zhou H Y, Zhang M, et al. A high sensitivity optical fiber sensor for GIS partial discharge detection[J]. IEEE Sensors Journal, 2019, 19(20): 9235-9243.

[3] Chen K, Guo M, Liu S, et al. Fiber-optic photoacoustic sensor for remote monitoring of gas micro-leakage[J]. Optics Express, 2019, 27(4): 4648-4659.

[4] Ma F X, Tian Y, Chen K, et al. Technique for detection of dissolved gas in oil based on miniature photoacoustic sensor[J]. Acta Optica Sinica, 2020, 40(7): 0730003.
马凤翔, 田宇, 陈珂, 等. 基于微型光声传感器的油中溶解气体检测技术[J]. 光学学报, 2020, 40(7): 0730003.

[5] Wei P, Han X L, Xia D. Measurement method for the velocity of acoustic emission wave in liquid nitrogen [J]. IEEE Transactions on Industrial Electronics, 2018, 65(10): 8232-8238.

[6] Gao C M, Nie F, Zhang P, et al. Optical fiber acoustic sensors [J]. Opto-Electronic Engineering, 2018, 45(9): 116-125.
高椿明, 聂峰, 张萍, 等. 光纤声传感器综述[J]. 光电工程, 2018, 45(9): 116-125.

[7] Xu Y P, Zhang L, Gao S, et al. Highly sensitive fiber random-grating-based random laser sensor for ultrasound detection[J]. Optics Letters, 2017, 42(7): 1353-1356.

[8] Qian S, Chen H, Xu Y, et al. High sensitivity detection of partial discharge acoustic emission within power transformer by Sagnac fiber optic sensor[J]. IEEE Transactions on Dielectrics and Electrical Insulation, 2018, 25(6): 2313-2320.

[9] Li S J, Liang J S, Wang F J, et al. Experiment of a single-mode fiber acoustic sensor based on Mach-Zehnder interferometer[J]. College Physics, 2011, 30(6): 52-56.
李双佶, 梁景舒, 王福娟, 等. 基于 Mach-Zehnder 干涉仪的单模光纤声波传感器的研究[J]. 大学物理, 2011, 30(6): 52-56.

[10] Wang Y J, Li F, Xiao H, et al. Fiber optic sound sensor based on Michelson interferometer[J]. Acta Photonica Sinica, 2009, 38(5): 1114-1117.
王永杰, 李芳, 肖浩, 等. Michelson 干涉仪式光纤空气声传感器[J]. 光子学报, 2009, 38(5): 1114-1117.

[11] Yang C, Fu H W, Yong Z, et al. Research on extrinsic fiber F-P interference acoustic sensor[J]. Optical Communication Technology, 2020, 44(2): 28-32.
杨冲, 傅海威, 雍振, 等. 非本征光纤 F-P 干涉声传感器的研究[J]. 光通信技术, 2020, 44(2): 28-32.

[12] Li H Z, Wu G M, Ma Z J, et al. Preparation of fiber-optic interferometer based infrasound sensor [J]. Laser & Optoelectronics Progress, 2019, 56(15): 150603.
李汉正, 吴高米, 马振钧, 等. 光纤干涉次声传感器研制[J]. 激光与光电子学进展, 2019, 56(15): 150603.

[13] Mao X F, Yuan S Z, Zheng P C, et al. Stabilized fiber-optic Fabry-Perot acoustic sensor based on improved wavelength tuning technique[J]. Journal of

Lightwave Technology, 2017, 35(11): 2311-2314.

[14] Ma J Y, Zhao M R, Huang X J, et al. Low cost, high performance white-light fiber-optic hydrophone system with a trackable working point[J]. Optics Express, 2016, 24(17): 19008-19019.

[15] Zhang Q, Zhu Y P, Luo X Y, et al. Acoustic emission sensor system using a chirped fiber-Bragg-grating Fabry-Perot interferometer and smart feedback control[J]. Optics Letters, 2017, 42(3): 631-634.

[16] Sun W, Yu M, Chang T Y, et al. Research and improvement based on PGC demodulation method [J]. Acta Photonica Sinica, 2018, 47(8): 0806004.
孙韦, 于淼, 常天英, 等. 相位生成载波解调方法的研究[J]. 光子学报, 2018, 47(8): 0806004.

[17] Liu Q, Jing Z G, Li A, et al. Common-path dual-wavelength quadrature phase demodulation of EFPI sensors using a broadly tunable MG-Y laser[J]. Optics Express, 2019, 27(20): 27873-27881.

[18] Jia J S, Jiang Y, Gao H C, et al. Three-wavelength passive demodulation technique for the interrogation of EFPI sensors with arbitrary cavity length[J]. Optics Express, 2019, 27(6): 8890-8899.

[19] Kim Y, Hibino K, Sugita N, et al. Measurement of optical thickness variation of BK_7 plate by wavelength tuning interferometry[J]. Optics Express, 2015, 23(17): 22928-22938.

[20] Ding Y, Chen L, Wang Z H, et al. Wavelength phase shifting interferometry based on current modulation[J]. Infrared and Laser Engineering, 2018, 47(5): 108-114.
丁煜, 陈磊, 王志华, 等. 电调谐波长移相干涉术[J]. 红外与激光工程, 2018, 47(5): 108-114.

[21] Liu Q, Jing Z G, Li A, et al. Multiplexing fiber-optic Fabry-Perot acoustic sensors using self-calibrating wavelength shifting interferometry[J]. Optics Express, 2019, 27(26): 38191-38203.

[22] Jang B W, Kim C G. Impact localization of composite stiffened panel with triangulation method using normalized magnitudes of fiber optic sensor signals [J]. Composite Structures, 2019, 211: 522-529.

[23] Wang J, Peng H K, Zhou P W, et al. Sound source localization based on Michelson fiber optic interferometer array[J]. Optical Fiber Technology, 2019, 51: 112-117.

[24] Jiao C, Zhang T, Sun J H. Convolutional neural network based indoor microphone array sound source localization[J]. Laser & Optoelectronics Progress, 2020, 57(8): 081021.
焦琛, 张涛, 孙建红. 基于卷积神经网络的室内麦克风阵列声源定位算法[J]. 激光与光电子学进展, 2020, 57(8): 081021.

[25] Lavrov V S, Plotnikov M Y, Aksarin S M, et al. Experimental investigation of the thin fiber-optic hydrophone array based on fiber Bragg gratings[J]. Optical Fiber Technology, 2017, 34: 47-51.

[26] Chen L, Huang J B. A real-time demodulation method of fiber Bragg grating sensor array[J]. Ship Electronic Engineering, 2008, 28(12): 185-188.
陈亮, 黄俊斌. 光纤布拉格光栅传感器阵列实时解调方案的研究[J]. 舰船电子工程, 2008, 28(12): 185-188.

[27] Hariharan P, Oreb B F, Eiju T. Digital phase-shifting interferometry: a simple error-compensating phase calculation algorithm[J]. Applied Optics, 1987, 26(13): 2504-2506.

[28] Slepneva S, Kovalev A, Rebrova N, et al. Coherence transfer in an akinetic swept source OCT laser with optical feedback[J]. Optics Letters, 2019, 44(21): 5161-5164.

[29] Park J, Carbajal E F, Chen X, et al. Phase-sensitive optical coherence tomography using an vernier-tuned distributed Bragg reflector swept laser in the mouse middle ear[J]. Optics Letters, 2014, 39(21): 6233-6236.

[30] Rohollahnejad J, Xia L, Cheng R, et al. TDM interrogation of intensity-modulated USFBGs network based on multichannel lasers[J]. Optics Express, 2017, 25(2): 670-680.

[31] Zuo C, Feng S J, Huang L, et al. Phase shifting algorithms for fringe projection profilometry: a review [J]. Optics and Lasers in Engineering, 2018, 109: 23-59.

[32] Jiang J F, Zhao Z X, Wang S, et al. Optical fiber Fabry-Perot interferometer based on phase-shifting technique and birefringence crystals[J]. Optics Express, 2018, 26(17): 21606-21614.

[33] Li D L, Cao Y P, Fu G K, et al. An improved 2+1 phase-shifting algorithm[J]. Optics Communications, 2019, 444: 165-171.

[34] Chang T Y, Lang J P, Sun W, et al. Phase compensation scheme for fiber-optic interferometric vibration demodulation[J]. IEEE Sensors Journal, 2017, 17(22): 7448-7454.

[35] Liu B, Lin J, Liu H, et al. Diaphragm based long cavity Fabry-Perot fiber acoustic sensor using phase generated carrier[J]. Optics Communications, 2017, 382: 514-518.

[36] Fu T, Liu YJ, Lau K T, et al. Impact source identification in a carbon fiber reinforced polymer plate by using embedded fiber optic acoustic emission sensors[J]. Composites Part B: Engineering, 2014, 66: 420-429.

Sound Source Localization System Based on Diaphragm-Type EFPI Optical Fiber Microphones

Xia Zhenjie[1], Liu Qiang[2], Li Ang[1], Liu Yueying[1], Jing Zhenguo[2], Peng Wei[2*]

[1] *School of Optoelectronic Engineering and Instrument Science, Dalian University of Technology, Dalian, Liaoning* 116024, *China*;

[2] *School of Physics, Dalian University of Technology, Dalian, Liaoning* 116024, *China*

Abstract

Objective Fiber-optic acoustic sensors play an important role in various fields owing to their unique features such as miniature size, antielectromagnetic interference, wide frequency response, and good performance in harsh environments. Diaphragm-based extrinsic Fabry-Perot interferometric (EFPI) acoustic sensors have attracted considerable interest owing to their high sensitivity and reflective-type sensor structure. Quadrature-point (Q-point)-based intensity detection is one of the most widely used demodulation techniques for EFPI acoustic sensors. However, the dynamic range of sound pressure detected by intensity is limited. Signal distortion occurs when detecting strong acoustic signals. Besides, the Q-points of different sensors are susceptible to external environmental fluctuations, thereby eliminating the possibility of multiplexing and multipoint detection. Phase-generated carrier (PGC) demodulation methods typically require a piezoelectric transducer (PZT) to generate the phase carrier; hence, such systems are bulky. In addition, the mechanical characteristics of the PZT will result in a limited frequency response range. Frequency- or wavelength-modulated phase-shifting interferometry (PSI) is a promising alternative for high-speed phase retrieval. The target quadrature phase shift is introduced by the frequency-or wavelength-tuning of a tunable laser, thereby avoiding the nonlinear errors caused by the phase shifters such as PZTs. For EFPI sensors with different cavity lengths, the phase shift can be calculated separately to achieve simultaneous demodulation. This creates the possibility of multiplexing and multipoint detection. Two-dimensional (2D) sound source localization is one of the most typical applications of multipoint acoustic detection. Compared with fiber Bragg grating (FBG) acoustic sensor, which suffers from the problem of low sensitivity, the fiber-optic EFPI acoustic sensor is more suitable for sound source localization and has the advantages of a probe-type structure and high sensitivity imparted by the high-performance and flexible multipoint demodulation techniques.

Methods Frequency-modulated quasicontinuous phase-shift interferometry (FMQC-PSI) was employed to construct a phase-demodulation system. An all-semiconductor programmable modulated grating Y-branch (MG-Y) tunable laser was used as the phase shifter. This laser has a frequency sweep range of 191.316–196.328 THz with a flat intensity output. Fast and stable frequency tuning was performed using a field-programmable gate array (FPGA) to introduce phase shifts. Four optical frequencies with $\pi/2$ phase bias were sequentially switched to generate quasicontinuous quadrature phase-shifted signals. Based on a stable 5-step phase-shifting algorithm, any five adjacent intensity signals were used to recover the time-varying phase signal modulated by the applied sound pressure. Thus, a phase sampling rate of 600 kHz was achieved during continuous frequency modulation. EFPI acoustic sensors with a wide cavity length range can be effectively demodulated by adjusting the four operating frequencies. Because of the absence of mechanical moving parts, high-speed and stable phase demodulation was realized.

Results and Discussions The FMQC-PSI system demodulated an EFPI fiber-optic microphone with a cavity length of 279.502 μm based on a PET diaphragm. It correctly recovered the phase signal of the applied acoustic signal at different sound pressures at a frequency of 3 kHz (Fig. 3). The demodulated phase signal had a good sinusoidal waveform, indicating the advantage of the system in detecting strong sound signals. At 3 kHz and 2.43 Pa, the signal-to-noise ratio (SNR) of the sensor output signal was calculated as 76.8 dB, with a background noise of 25.4 dB (Fig. 4). The sensitivity of the sensor is 0.63 rad/Pa when the applied sound pressure amplitude varied between 0.75 Pa and 2.43 Pa, good linearity is observed in this range. The frequency response characteristic curve of the sensor in the frequency range of 1–10 kHz was obtained (Fig. 5). Moreover, the system can correctly demodulate EFPI sensors with different cavity lengths and frequencies (Fig. 6). In the 2D sound source localization experiment, a four-sensor sound source localization system was constructed. The hyperbolic positioning algorithm is used to estimate the sound source position. The time difference of arrival (TDOA) measured by the two pairs of sensors

along the orthogonal axis is used to determine the two hyperbolas. When the point sound source was placed at the coordinates of (30 cm, −15 cm), the localization result of the sound source position was estimated as (30.01 cm, −15.82 cm), which is in good agreement with the actual position. Six repeated measurements at 25 different positions were performed to test its positioning accuracy. The positioning results at the same sound source position were found to be highly consistent, and the positioning errors of all measurements were not larger than 1.98 cm (Fig. 9).

Conclusions In this study, a frequency-modulated quadrature phase-shifted demodulation technique was used to demodulate the phase of diaphragm EFPI optical fiber microphone, and its application for sound source localization was demonstrated. Quasicontinuous phase-shifted signals were generated by the sequential modulation of four laser frequencies with $\pi/2$ phase differences. The phase sampling rate depends on the frequency tuning rate of the laser up to 600 kHz. Owing to the wide frequency tuning range (191.316–196.328 THz), EFPI acoustic sensors with different cavity lengths (33.518–745.504 μm) can be demodulated by adjusting the specific values of the four laser frequencies. In addition, the simultaneous demodulation of multiple acoustic sensors can be easily achieved by space division multiplexing. We built a compact four-sensor FMQC-PSI system for 2D sound source localization. The experimental results demonstrated the effectiveness of this method.

Key words measurement; phase measurement; phase shift interferometry; modulated grating Y-branch laser; optical fiber microphone; sound source localization

OCIS codes 120.5050; 140.5960; 280.4788